arXiv:hep-ph/0210138v7 17 Nov 2003

Flavor changing neutrino interactions and CP violation in neutrino oscillations

Toshihiko Hattori,[a),1] Tsutom Hasuike,[b),2] and Seiichi Wakaizumi[c),3]

[a)] *Institute of Theoretical Physics, University of Tokushima, Tokushima 770-8502, Japan*
[b)] *Department of Physics, Anan College of Technology, Anan 774-0017, Japan*
[c)] *Center for University Extension, University of Tokushima, Tokushima 770-8502, Japan*

Abstract

We investigate the interference effects of non-standard neutrino-matter interactions (NSNI) with the mass-induced neutrino oscillations. The NSNI is composed of flavor-changing neutrino interactions (FCNI) and flavor-diagonal neutrino interactions (FDNI). Both of the interactions are introduced in the $\nu_\mu - \nu_\tau$ sector and the $\nu_e - \nu_\mu$ sector in order to study their effects in $\nu_\mu \to \nu_\tau$ and $\nu_\mu \to \nu_e$ oscillations, respectively. The FCNI effect proves to possibly dominate the CP violating effect and significantly survive as a fake CP violating effect in the neutrino energy region where the pure CP violating effect, ordinary matter effect and FDNI effect fall, for example, above 4 GeV at the baseline of $L = 730$ km in the $\nu_\mu \to \nu_\tau$ oscillation for the maximum parameter values of FCNI and FDNI allowed by the atmospheric neutrino oscillation data. The FCNI and FDNI effects on CP violation in $\nu_\mu \to \nu_e$ oscillation are negligibly small due to the stringent constraints on FCNI from the bounds on lepton flavor violating processes and on FDNI from the limits on lepton universality violation.

---

[1] e-mail: hattori@ias.tokushima-u.ac.jp
[2] e-mail: hasuike@anan-nct.ac.jp
[3] e-mail: wakaizum@cue.tokushima-u.ac.jp

I Introduction

In the framework of massive neutrinos and leptonic mixing, the atmospheric neutrino anomaly [1] is resolved by the $\nu_\mu \to \nu_\tau$ oscillation with nearly maximal mixing [2] and the solar neutrino deficit [3] is interpreted by the oscillation of ν_e into another neutrino state with large mixing angle solution [4] in the Mikheyev-Smirnov-Wolfenstein (MSW) mechanism of neutrino interactions with matter [5] in the three-neutrino scheme, where the neutrino flavor eigenstates ν_α $(\alpha = e, \mu, \tau)$ are expressed by a superposition of their mass eigenstates ν_i $(i = 1, 2, 3)$ with mass m_i as follows:

$$\nu_\alpha = \sum_{i=1}^{3} U_{\alpha i}\, \nu_i, \tag{1}$$

where U is the 3×3 unitary mixing matrix, which is called as Maki-Nakagawa-Sakata (MNS) matrix [6]. The reactor experiment of search for $\bar{\nu_e}$ oscillations, CHOOZ, gives an upper limit on the element U_{e3}, which is very small as $|U_{e3}| < 0.22$ [7]. The liquid scintillation experiment, LSND, claims a discovery of $\bar{\nu_\mu} \to \bar{\nu_e}$ oscillations [8], which requires a fourth sterile neutrino.

The above situation seems to convince us of a scheme of massive neutrinos and lepton mixing. In addition to this scheme, it is interesting to investigate non-standard neutrino-matter interactions in the neutrino oscillations in order to search for new physics beyond the standard model. The non-standard neutrino-matter interaction (NSNI) is originated from Wolfenstein's work [9] and the flavor-changing neutrino-matter interaction (FCNI) and flavor-diagonal neutrino-matter interaction (FDNI) were used in order to study the solar neutrino problem, not by relying on the mass-induced neutrino oscillations [10][11], and then by considering them as sub-leading effects to the standard mass-induced oscillations [12]. For the atmospheric neutrino problem, the FDNI alone [13] and both of the FCNI and FDNI were applied [14]. The mere NSNI, however, has proved not to be able to solve the atmospheric neutrino problem [15][16].

After that, the FCNI has been studied as sub-leading effects to the standard mass-induced neutrino oscillations by considering FCNI in $\nu_\mu - \nu_\tau$ sector and in $\nu_e - \nu_\tau$ sector [16][17] and its detectability at a future neutrino factory is discussed in Refs.[17] [18][19]. In Ref.19, it is shown that the FCNI dominates the ν_e oscillation probability at sufficiently high neutrino energies. Moreover, the NSNI with the netrino masses can induce some fake CP violating effect in matter in the long-baseline oscillation experiments [20]. There are also combined analyses with new flavor-changing neutrino interactions occuring in the neutrino production and detection processes in addition to the above-mentioned non-standard interactions with matter during neutrino propagation, of which effects are enhanced by the interference with the ordinary weak interactions in the oscillation phenomena [21].

In this paper, we analyze the non-standard neutrino-matter interaction effects (NSNI) to the CP violating effects in the neutrino oscillations by considering them in $\nu_\mu - \nu_\tau$ sector and $\nu_e - \nu_\mu$ sector in the three-neutrino scheme. The NSNI consists of the above-mentioned FCNI and flavor-diagonal neutrino-matter interactions (FDNI). The evolution equation of the neutrino flavor states is solved analytically by using Arafune-Koike-Sato's perturbative method [22] and we calculate the neutrino oscillation probability for the general $\nu_\alpha \to \nu_\beta$ oscillation. We apply this analytic expression of the probability to calculate the CP violating effects in $\nu_\mu \to \nu_\tau$ and $\nu_\mu \to \nu_e$ oscillations, *i.e.* the difference between the neutrino and the antineutrino oscillation probabilities. We find that the FCNI matter effect survives and dominates the CP violating effect in $\nu_\mu \to \nu_\tau$ oscillation even after both the pure CP violating effect due to the phase of U and the fake CP violating ones due to the ordinary and FDNI matter effects fall. This shows that the non-standard flavor changing neutrino-matter interaction could be detected in the CP violating effect in $\nu_\mu \to \nu_\tau$ oscillation at the neutrino energies where both the pure CP violating effect and the ordinary matter effect become sufficiently small and undetectable. For $\nu_\mu \to \nu_e$ oscillation, the FCNI and FDNI effects on the CP violating effect are negligibly small due to the stringent constraints [11][15][23] on FCNI from the bounds on lepton flavor violating processes and on FDNI from the limits on lepton universality violation.

The paper is organized as follows. In Sec. II the oscillation probability is derived by solving analytically the evolution equation of the neutrino flavor states with the non-standard neutrino-matter interactions in $\nu_\mu - \nu_\tau$ sector. The effect of the NSNI is studied in the CP violating effects in the $\nu_\mu \to \nu_\tau$ oscillation. In Sect. III the same will be done for the NSNI in $\nu_e - \nu_\mu$ sector and the effect of the NSNI is studied in the CP violating effects in the $\nu_\mu \to \nu_e$ oscillation. Section IV is devoted to the conclusions and discussions.

II Oscillation probability and CP violating effect with NSNI in $\nu_\mu - \nu_\tau$ sector

Here and in the next section we calculate the neutrino oscillation probabilities and CP violating effects with the inclusion of the NSNI in $\nu_\mu - \nu_\tau$ sector and in $\nu_e - \nu_\mu$ sector, respectively, in the three-neutrino scheme by solving analylitically the evolution equation for neutrino flavor states in the perturbative method.

If we consider the effect of NSNI in the $\nu_\mu - \nu_\tau$ sector, the evolution equation in matter is given as

$$i\,\frac{d}{dx}\begin{pmatrix}\nu_e\\ \nu_\mu\\ \nu_\tau\end{pmatrix} = H\begin{pmatrix}\nu_e\\ \nu_\mu\\ \nu_\tau\end{pmatrix}, \tag{2}$$

and [17]

$$H = \frac{1}{2E}U\begin{pmatrix}0 & 0 & 0\\ 0 & \Delta m^2_{21} & 0\\ 0 & 0 & \Delta m^2_{31}\end{pmatrix}U^\dagger + \begin{pmatrix}V_e(x) & 0 & 0\\ 0 & 0 & \epsilon^f_{\mu\tau}V_f(x)\\ 0 & \epsilon^{f*}_{\mu\tau}V_f(x) & \epsilon'^f_{\mu\tau}V_f(x)\end{pmatrix}, \tag{3}$$

where E is the neutrino energy, $\Delta m^2_{ij} = m^2_i - m^2_j$, m_i being the mass of i-th neutrino, U is the MNS leptonic mixing matrix, $V_f(x) = \sqrt{2}G_F n_f(x)$, x being the position of the running neutrino, $\epsilon^f_{\mu\tau} V_f(x)$ is the flavor-changing $\nu_\mu + f \to \nu_\tau + f$ forward scattering amplitude due to the flavor-changing neutrino-matter interaction(FCNI), and $\epsilon'^f_{\mu\tau} V_f(x)$ is the difference between the flavor-diagonal $\nu_\mu - f$ and $\nu_\tau - f$ elastic forward scattering amplitudes due to the flavor-diagonal neutrino-matter interaction(FDNI), with $n_f(x)$ being the number density of the fermion $f (f = u, d, e)$ which induces such processes. In Eq.(3), $\epsilon^f_{\mu\tau}$ and $\epsilon'^f_{\mu\tau}$ are the phenomenological parameters which characterize the strength of FCNI and FDNI, respectively. The fermion number density $n_f(x)$ can be written in terms of the matter density ρ as $n_f(x) = \rho(x) Y_f$, where Y_f is the fraction of the fermion f per nucleon, $\sim 1/2$ for electrons and $\sim 3/2$ for u or d quarks. In the following, we consider interactions only with either u or d quarks, since for the NSNI with electrons the same effects presented in this paper can be obtained simply by increasing the parameters $\epsilon^{u,d}_{\mu\tau}$ and $\epsilon'^{u,d}_{\mu\tau}$ by a factor 3.

For the evolution equation of the antineutrinos, the replacement of $U \to U^*, V_{e,f}(x) \to -V_{e,f}(x)$ and $\epsilon^f_{\mu\tau} \to \epsilon^{f*}_{\mu\tau}$ should be done in Eq.(3).

We use here Arafune-Koike-Sato's perturbative method to solve analytically the evolution equation [22]. The solution of Eq.(2) is given by

$$\nu(x) = S(x)\nu(0), \tag{4}$$

with

$$S(x) = T\exp\left(-i \int_0^x ds H(s)\right), \tag{5}$$

where

$$\nu(x) = \begin{pmatrix} \nu_e(x) \\ \nu_\mu(x) \\ \nu_\tau(x) \end{pmatrix} \tag{6}$$

and T is the time ordering operator. In the following, the oscillation probability and the CP violating effect are calculated for the baseline of $L = 300$ and 730 km so that we assume $n_f(x)$ and $\rho(x)$ to be independent of x. Then we have

$$S(x) = e^{-iHx}. \tag{7}$$

The oscillation probability for $\nu_\alpha \to \nu_\beta$ at the distance L from the neutrino production point is given in terms of S in Eq.(5) as follows:

$$P(\nu_\alpha \to \nu_\beta; L) = |S_{\beta\alpha}(L)|^2 . \tag{8}$$

We express the Hamiltonian H of Eq.(3) for simplicity as

$$H = \frac{1}{2E} U \begin{pmatrix} 0 & 0 & 0 \\ 0 & \Delta m_{21}^2 & 0 \\ 0 & 0 & \Delta m_{31}^2 \end{pmatrix} U^\dagger + \frac{1}{2E} \begin{pmatrix} a & 0 & 0 \\ 0 & 0 & \epsilon b \\ 0 & \epsilon^* b & \epsilon' b \end{pmatrix} , \tag{9}$$

where

$$a \equiv 2EV_e = 2\sqrt{2} G_F n_e E = 7.60 \times 10^{-5} \frac{\rho}{[\mathrm{g\,cm^{-3}}]} \frac{E}{[\mathrm{GeV}]} \ \mathrm{eV}^2, \tag{10}$$

$$\epsilon b \equiv 2E\epsilon_{\mu\tau}^f V_f = 15.2 \times 10^{-5} \epsilon Y_f \frac{\rho}{[\mathrm{g\,cm^{-3}}]} \frac{E}{[\mathrm{GeV}]} \ \mathrm{eV}^2, \tag{11}$$

$$\epsilon' b \equiv 2E\epsilon'^f_{\mu\tau} V_f = 15.2 \times 10^{-5} \epsilon' Y_f \frac{\rho}{[\mathrm{g\,cm^{-3}}]} \frac{E}{[\mathrm{GeV}]} \ \mathrm{eV}^2, \tag{12}$$

where $\epsilon_{\mu\tau}^f$ and $\epsilon'^f_{\mu\tau}$ are denoted as ϵ and ϵ', respectively, and $2EV_f$ is denoted as b, for brevity. In general, ϵ is complex and ϵ' is real from the hermeticity of the Hamiltonian. Since $\Delta m_{21}^2 \ll \Delta m_{31}^2$ and $a, |\epsilon| b, |\epsilon'| b \ll \Delta m_{31}^2$ because of $|\epsilon| < 0.02$ and $|\epsilon'| < 0.05$ from the analysis of the atmospheric neutrino problem [16], we decompose H of Eq.(9) as $H = H_0 + H_1$ with

$$H_0 = \frac{1}{2E} U \begin{pmatrix} 0 & 0 & 0 \\ 0 & 0 & 0 \\ 0 & 0 & \Delta m_{31}^2 \end{pmatrix} U^\dagger, \tag{13}$$

and

$$H_1 = \frac{1}{2E} U \begin{pmatrix} 0 & 0 & 0 \\ 0 & \Delta m_{21}^2 & 0 \\ 0 & 0 & 0 \end{pmatrix} U^\dagger + \frac{1}{2E} \begin{pmatrix} a & 0 & 0 \\ 0 & 0 & \epsilon b \\ 0 & \epsilon^* b & \epsilon' b \end{pmatrix} , \tag{14}$$

and treat H_1 as a perturbation and calculate Eq.(7) up to the first order in $\Delta m_{21}^2, a, \epsilon b$ and $\epsilon' b$. Then, $S(x)$ is given by

$$S(x) \simeq e^{-i H_0 x} - i\, e^{-i H_0 x} \int_0^x ds H_1(s), \tag{15}$$

where $H_1(x) = e^{i\,H_0 x} H_1\, e^{-i\,H_0 x}$. The approximation in Eq.(15) requires

$$\frac{\Delta m^2_{21} L}{2E} \ll 1, \qquad \frac{|\epsilon| b L}{2E} \ll 1, \qquad \frac{\epsilon' b L}{2E} \ll 1. \tag{16}$$

The requirements of Eq.(16) are satisfied for $\Delta m^2_{21} = (10^{-5} - 10^{-4})\ \mathrm{eV}^2, E = 1-20$ GeV, $L = (300 - 730)$ km, $\rho = 3\mathrm{g/cm}^3$, $|\epsilon| \sim 0.02$ and $|\epsilon'| \sim 0.05$ as

$$\begin{aligned}\frac{\Delta m^2_{21} L}{2E} &\simeq 4 \times 10^{-4} - 0.2, \qquad \frac{|\epsilon| b L}{2E} \simeq (1 - 2.5) \times 10^{-2}, \\ \frac{|\epsilon'| b L}{2E} &\simeq (2.5 - 6) \times 10^{-2}.\end{aligned} \tag{17}$$

Equation (16) also shows that the approximation becomes better as the energy E increases. If we express $S_{\beta\alpha}(x)$ as

$$S_{\beta\alpha}(x) = \delta_{\beta\alpha} + i\,T_{\beta\alpha}(x), \tag{18}$$

then $i\,T_{\beta\alpha}(x)$ is obtained as follows:

$$\begin{aligned} i\,T_{\beta\alpha}(x) &= -2\,i \exp\left(-i\,\frac{\Delta m^2_{31} x}{4E}\right) \sin\left(\frac{\Delta m^2_{31} x}{4E}\right) \Big[\, U_{\beta 3} U^*_{\alpha 3} \{1 - \frac{a}{\Delta m^2_{31}} (2|U_{e3}|^2 \\ &\quad - \delta_{\alpha e} - \delta_{\beta e}) - i\,\frac{ax}{2E} |U_{e3}|^2 - \frac{\epsilon' b}{\Delta m^2_{31}} (2|U_{\tau 3}|^2 - \delta_{\alpha\tau} - \delta_{\beta\tau}) \\ &\quad - i\,\frac{\epsilon' b x}{2E} |U_{\tau 3}|^2\} - \frac{1}{\Delta m^2_{31}} \{4 U^*_{\alpha 3} U_{\beta 3} \mathrm{Re}(\epsilon b U^*_{\mu 3} U_{\tau 3}) \\ &\quad - \epsilon^* b (U^*_{\alpha 3} U_{\mu 3} \delta_{\beta\tau} + U_{\beta 3} U^*_{\tau 3} \delta_{\alpha\mu}) - \epsilon b (U^*_{\alpha 3} U_{\tau 3} \delta_{\beta\mu} \\ &\quad + U_{\beta 3} U^*_{\mu 3} \delta_{\alpha\tau})\} - 2\,i\,\frac{x}{2E} U^*_{\alpha 3} U_{\beta 3} \mathrm{Re}(\epsilon b U^*_{\mu 3} U_{\tau 3})\, \Big] \\ &\quad - i\,\frac{\Delta m^2_{31} x}{2E} \Big[\, \frac{\Delta m^2_{21}}{\Delta m^2_{31}} U_{\beta 2} U^*_{\alpha 2} + \frac{a}{\Delta m^2_{31}} \{\delta_{\alpha e} \delta_{\beta e} + U_{\beta 3} U^*_{\alpha 3} (2|U_{e3}|^2 - \delta_{\alpha e} \\ &\quad - \delta_{\beta e})\} + \frac{\epsilon' b}{\Delta m^2_{31}} \{\delta_{\alpha\tau} \delta_{\beta\tau} + U_{\beta 3} U^*_{\alpha 3} (2|U_{\tau 3}|^2 - \delta_{\alpha\tau} - \delta_{\beta\tau})\} \\ &\quad + \frac{1}{\Delta m^2_{31}} \{\epsilon^* b \delta_{\beta\tau} \delta_{\alpha\mu} + \epsilon b \delta_{\beta\mu} \delta_{\alpha\tau} + 4 U^*_{\alpha 3} U_{\beta 3} \mathrm{Re}(\epsilon b U^*_{\mu 3} U_{\tau 3}) \\ &\quad - \epsilon^* b (U^*_{\alpha 3} U_{\mu 3} \delta_{\beta\tau} + U_{\beta 3} U^*_{\tau 3} \delta_{\alpha\mu}) - \epsilon b (U^*_{\alpha 3} U_{\tau 3} \delta_{\beta\mu} \\ &\quad + U_{\beta 3} U^*_{\mu 3} \delta_{\alpha\tau})\}\, \Big]. \end{aligned} \tag{19}$$

We use Eq.(19) in Eq.(18) and calculate the oscillation probability for $\nu_\alpha \to \nu_\beta$ by Eq.(8). The complete expression of $P(\nu_\alpha \to \nu_\beta; L)$ with the NSNI in $\nu_\mu - \nu_\tau$ sector is given in the Appendix A.

Now we will study the effects due to the NSNI in $\nu_\mu - \nu_\tau$ sector on the oscillation probability and the CP violating effect in $\nu_\mu \to \nu_\tau$ oscillation at the baseline of $L = 730$ km. For the MNS mixing matrix U, we take the standard parametrization given by

$$U = \begin{pmatrix} c_{12}c_{13} & s_{12}c_{13} & s_{13}e^{-i\,\delta} \\ -s_{12}c_{23} - c_{12}s_{23}s_{13}e^{i\,\delta} & c_{12}c_{23} - s_{12}s_{23}s_{13}e^{i\,\delta} & s_{23}c_{13} \\ s_{12}s_{23} - c_{12}c_{23}s_{13}e^{i\,\delta} & -c_{12}s_{23} - s_{12}c_{23}s_{13}e^{i\,\delta} & c_{23}c_{13} \end{pmatrix}, \qquad (20)$$

where $c_{ij} = \cos\theta_{ij}, s_{ij} = \sin\theta_{ij}$ and δ is the CP violating phase. From the Super-Kamiokande data for the atmospheric neutrino oscillation [2], $\sin^2 2\theta_{\rm atm} > 0.82$ and $5 \times 10^{-4} < \Delta m^2_{\rm atm} < 6 \times 10^{-3}$ eV^2, we take in the following $\sin\theta_{23} = 0.707$ for the mixing angle s_{23} and $\Delta m^2_{31} = 2.5 \times 10^{-3}$ eV^2 as a typical value. For s_{12}, we take $\sin\theta_{12} = 0.54$ and $\Delta m^2_{21} = 7.3 \times 10^{-5}$ eV^2 from the presently most probable large-mixing angle solution (LMA) to the solar neutrino oscillation [24]. For s_{13}, we tentatively assume $\sin\theta_{13} = 0.14$ from the CHOOZ data on $\bar{\nu}_e$ oscillation [7], $\sin^2 2\theta_{\rm CHOOZ} < 0.18$ for $3 \times 10^{-3} < \Delta m^2 < 1.0 \times 10^{-2}$ eV^2, which means $0 < \sin\theta_{13} < 0.22$. For the phenomenological parameters of the NSNI, the constraints are derived to be $-0.03 < \epsilon < 0.02$ and $|\epsilon'| < 0.05$ from the analyses of the atmospheric neutrino data by Fonengo et al. [16]. They assumed ϵ to be real. Here we generally take ϵ to be complex. For the numerical calculations we take $|\epsilon| = 0.01$ and $\epsilon' = \pm 0.02$, and the effects of the FCNI on CP violation have proved to be maximum at $\phi = 0$ and π for the phase of ϵ, $\epsilon = |\epsilon|\, e^{i\phi}$.

In the following, we present the numerical results for the oscillation probabilities and CP violating effects in the $\nu_\mu \to \nu_\tau$ oscillation. The effect of NSNI in the $\nu_\mu - \nu_\tau$ sector is not so significant in the $\nu_\mu \to \nu_e$ and $\nu_e \to \nu_\tau$ oscillations as in the $\nu_\mu \to \nu_\tau$ oscillation. Fig.1 and Fig.2 show the $\nu_\mu \to \nu_\tau$ oscillation probabilities for $|\epsilon| = 0.01, \epsilon' = 0.02, \delta = \pi/2, \Delta m^2_{31} > 0$ for the neutrino energy range of $E = 1 - 20$ GeV at the baseline of $L = 730$ km for $\phi = 0$ (Fig.1) and $\phi = \pi$ (Fig.2), respectively, where the solid line represents the oscillation probability including all the three matter effects, *i.e.* ordinary matter effect (denoted as

a in Eq.(14)), flavor-changing neutrino-matter interaction (FCNI, denoted as ϵb) and flavor-diagonal neutrino-matter interaction (FDNI, denoted as $\epsilon' b$), and the dashed line represents the one without any matter effects. These two Figures show that the matter effects due to the NSNI are small for the oscillation probability.

Figs.3-6 show the CP violating effects in the $\nu_\mu \to \nu_\tau$ oscillation, calculated as the difference between the neutrino and the antineutrino oscillation probabilities, for the energy range of $E = 1 - 20$ GeV at the baseline of $L = 730$ km. The phase of the MNS mixing matrix U is taken as $\delta = \pi/2$. The dash-dotted line is the pure CP violating effect due to the phase of U. The long-dashed, short-dashed and dotted lines are the fake CP violating effects due to the ordinary, FCNI and FDNI matter effects, respectively. The solid line represents the total CP violating effect with the sum of the pure and fake ones. For Fig.3-6, we have taken $|\epsilon| = 0.01, |\epsilon'| = 0.02$ and $|\Delta m^2_{31}| = 2.5 \times 10^{-3}$ eV^2. In Fig.3, the phase of ϵ is taken as $\phi = 0$ and $\epsilon' = +0.02$ (> 0) and $\Delta m^2_{31} > 0$. In Fig.4, $\phi = \pi, \epsilon' = +0.02$ and $\Delta m^2_{31} > 0$. In Fig.5, $\phi = 0, \epsilon' > 0$ and $\Delta m^2_{31} < 0$, and in Fig.6, $\phi = \pi, \epsilon' > 0$ and $\Delta m^2_{31} < 0$. As can be seen from these Figures, the FCNI matter effect dominates the CP violating effect in the whole range of $E = 1 - 20$ GeV, and all the other contributions of pure CP violation, ordinary matter effect and FDNI effect rapidly fall around 4 GeV and the FCNI effect survives significantly above this energy. When the sign of Δm^2_{31} is changed, the contributions of all the matter effects including FCNI and FDNI change the sign, as can be seen from the comparison of Fig.3 and Fig.5 and from Fig.4 and Fig.6.

Next we will show how much the predicted CP violation depends on the oscillation parameters in their allowed ranges. Fig.7 and Fig.8 give the dependence of the total CP violating effect in $\nu_\mu \to \nu_\tau$ oscillation at $L = 730$ km on the mass-squared differences Δm^2_{31} and Δm^2_{21} for $\Delta m^2_{31} = 1.5 \times 10^{-3}, 2.5 \times 10^{-3}, 3.5 \times 10^{-3}$ eV^2 and $\Delta m^2_{21} = 6 \times 10^{-5}, 7 \times 10^{-5}, 8 \times 10^{-5}$ eV^2, respectively. The dependence on Δm^2_{31} is large and that on Δm^2_{21} is very small, because the baseline of $L = 730$ km corresponds to the atmospheric neutrino mass scale. The dash-dotted curve in both Figures represents the pure CP violating effect without the FCNI and FDNI. Figs. 9, 10 and 11 give the dependence of the total CP violating effect on the mixing angles s_{23}, s_{12}, and s_{13} for $s_{23} = 0.55, 0.60, 0.65, s_{12} = 0.50, 0.55, 0.60$ and $s_{13} = 0.05, 0.10, 0.15$, respectively. The dependence on the mixing angles is evidently small. Again, the dash-dotted curve represents the pure CP violating effect without the FCNI and FDNI. These Figures 7-11 show that the new CP violating effects are significantly larger than the pure CP violating one coming from the standard model.

III NSNI in $\nu_e - \nu_\mu$ sector

In this section, we consider the NSNI in $\nu_e - \nu_\mu$ sector and study its effect on the CP violating effect in $\nu_\mu \rightarrow \nu_e$ oscillation at the baselines of $L = 300$ km.

The Hamiltonian of the evolution equation of the flavor neutrino states is given as

$$H = \frac{1}{2E} U \begin{pmatrix} 0 & 0 & 0 \\ 0 & \Delta m^2_{21} & 0 \\ 0 & 0 & \Delta m^2_{31} \end{pmatrix} U^\dagger + \begin{pmatrix} V_e(x) & \epsilon^f_{e\mu} V_f(x) & 0 \\ \epsilon^{f*}_{e\mu} V_f(x) & \epsilon'^f_{e\mu} V_f(x) & 0 \\ 0 & 0 & 0 \end{pmatrix}, \tag{21}$$

where $\epsilon^f_{e\mu} V_f(x)$ is the flavor-changing $\nu_e + f \rightarrow \nu_\mu + f$ forward scattering amplitude due to the FCNI and $\epsilon'^f_{e\mu} V_f(x)$ is the difference between the flavor-diagonal $\nu_e - f$ and $\nu_\mu - f$ elastic forward scattering amplitudes due to the FDNI. As in the previous section, we assume the matter density to be constant for the baseline of $L = 300$ km and reexpress Eq.(21) as

$$H = \frac{1}{2E} U \begin{pmatrix} 0 & 0 & 0 \\ 0 & \Delta m^2_{21} & 0 \\ 0 & 0 & \Delta m^2_{31} \end{pmatrix} U^\dagger + \frac{1}{2E} \begin{pmatrix} a & \eta b & 0 \\ \eta^* b & \eta' b & 0 \\ 0 & 0 & 0 \end{pmatrix}, \tag{22}$$

where a is the same as in Eq.(10) and

$$\eta b \equiv 2E \epsilon^f_{e\mu} V_f = 15.2 \times 10^{-5} \eta Y_f \frac{\rho}{[\mathrm{g\,cm^{-3}}]} \frac{E}{[\mathrm{GeV}]} \ \mathrm{eV}^2, \tag{23}$$

$$\eta' b \equiv 2E\epsilon'^{f}_{e\mu}V_f = 15.2\times 10^{-5}\eta' Y_f \frac{\rho}{[\mathrm{g\,cm^{-3}}]}\frac{E}{[\mathrm{GeV}]}\ \ \mathrm{eV}^2, \tag{24}$$

where $\epsilon^{f}_{e\mu}$ and $\epsilon'^{f}_{e\mu}$ are denoted as η and η', respectively, and $2EV_f$ is denoted as b, for brevity. In general, η is complex and η' is real. The experimental limits on various lepton flavor violating processes and $SU(2)_L$ breaking effects give a stringent constraint on the FCNI parameter as $|\eta| < 7\times 10^{-5}$ [11][15][23] and the upper bounds on lepton universality violation give a constraint on the FDNI parameter as $|\eta'| < 0.1$ [11][15]. So, we can decompose H of Eq.(22) as $H = H_0 + H_1$ with

$$H_1 = \frac{1}{2E}U\begin{pmatrix} 0 & 0 & 0 \\ 0 & \Delta m^2_{21} & 0 \\ 0 & 0 & 0 \end{pmatrix}U^\dagger + \frac{1}{2E}\begin{pmatrix} a & \eta b & 0 \\ \eta^* b & \eta' b & 0 \\ 0 & 0 & 0 \end{pmatrix}, \tag{25}$$

and treat H_1 as a perturbation. H_0 is the same as in Eq.(13). In the same way as for the NSNI in $\nu_\mu - \nu_\tau$ sector, we calculate $S(x)$ of Eq.(7) up to the first order in $\Delta m^2_{21}, a, \eta b$ and $\eta' b$ to obtain the expression of $i\,T_{\beta\alpha}(x)$ in Eq.(18):

$$\begin{aligned} i\,T_{\beta\alpha}(x) \;=\; & -2\,i\exp\left(-i\,\frac{\Delta m^2_{31}x}{4E}\right)\sin\left(\frac{\Delta m^2_{31}x}{4E}\right)\Big[\,U_{\beta3}U^*_{\alpha3}\{1-\frac{a}{\Delta m^2_{31}}(2|U_{e3}|^2 \\ & -\delta_{\alpha e}-\delta_{\beta e}) - i\,\frac{ax}{2E}|U_{e3}|^2 - \frac{\eta' b}{\Delta m^2_{31}}(2|U_{\mu3}|^2-\delta_{\alpha\mu}-\delta_{\beta\mu}) \\ & - i\,\frac{\eta' bx}{2E}|U_{\mu3}|^2\} - \frac{1}{\Delta m^2_{31}}\{4U^*_{\alpha3}U_{\beta3}\mathrm{Re}(\eta b U^*_{e3}U_{\mu3}) \\ & -\eta^* b(U^*_{\alpha3}U_{e3}\delta_{\beta\mu}+U_{\beta3}U^*_{\mu3}\delta_{\alpha e}) - \eta b(U^*_{\alpha3}U_{\mu3}\delta_{\beta e} \\ & + U_{\beta3}U^*_{e3}\delta_{\alpha\mu})\} - 2\,i\,\frac{x}{2E}U^*_{\alpha3}U_{\beta3}\mathrm{Re}(\eta b U^*_{e3}U_{\mu3})\,\Big] \\ & - i\,\frac{\Delta m^2_{31}x}{2E}\Big[\,\frac{\Delta m^2_{21}}{\Delta m^2_{31}}U_{\beta2}U^*_{\alpha2} + \frac{a}{\Delta m^2_{31}}\{\delta_{\alpha e}\delta_{\beta e}+U_{\beta3}U^*_{\alpha3}(2|U_{e3}|^2-\delta_{\alpha e} \\ & -\delta_{\beta e})\} + \frac{\eta' b}{\Delta m\ 2_{31}}\{\delta_{\alpha\mu}\delta_{\beta\mu}+U_{\beta3}U^*_{\alpha3}(2|U_{\mu3}|^2-\delta_{\alpha\mu}-\delta_{\beta\mu})\} \\ & + \frac{1}{\Delta m^2_{31}}\{\eta^* b\delta_{\beta\mu}\delta_{\alpha e}+\eta b\delta_{\beta e}\delta_{\alpha\mu}+4U^*_{\alpha3}U_{\beta3}\mathrm{Re}(\eta b U^*_{e3}U_{\mu3}) \\ & -\eta^* b(U^*_{\alpha3}U_{e3}\delta_{\beta\mu}+U_{\beta3}U^*_{\mu3}\delta_{\alpha e}) - \eta b(U^*_{\alpha3}U_{\mu3}\delta_{\beta e} \\ & + U_{\beta3}U^*_{e3}\delta_{\alpha\mu})\}\,\Big]. \end{aligned} \tag{26}$$

Using Eq.(26) in Eq.(18), we calculate the oscillation probability for $\nu_\alpha \to \nu_\beta$ by

Eq.(8). The complete expression of $P(\nu_\alpha \to \nu_\beta; L)$ with the NSNI in $\nu_e - \nu_\mu$ sector is given in the Appendix B.

Now we will study the effects due to the NSNI in $\nu_e - \nu_\mu$ sector on the CP violating effect in $\nu_\mu \to \nu_e$ oscillation at the baseline of $L = 300$ km. The values of the parameters $\Delta m^2_{21}, \Delta m^2_{31}, s_{23}, s_{12}$ and s_{13} are taken to be the same as in the previous section. The effect of the FCNI on CP violation has proved to be maximum at $\gamma = \pi/2$ and $3\pi/2$ for the phase of $\eta, \eta = |\eta| \mathrm{e}^{i\gamma}$. We present the numerical results for the CP violating effects in the $\nu_\mu \to \nu_e$ oscillation for the parameters satisfying the constraints. In Fig.12 we show the CP violating effect in $\nu_\mu \to \nu_e$ oscillation for $|\eta| = 7 \times 10^{-5}, \gamma = \pi/2, \eta' = 0.01$ in the neutrino energy range of $E = 0.3 - 2$ GeV at the baseline of $L = 300$ km for $\Delta m^2_{31} > 0$ and $\delta = \pi/2$ for the phase of U. The dash-dotted line represents the pure CP violating effect due to the phase of U. The long-dashed and short-dashed lines are the fake CP violating effects due to the ordinary and FCNI matter effects, respectively. The solid line represents the total CP violating effect, which is the sum of the pure and fake ones. The FCNI effect turns out to be negligibly small, so that the total CP violating effect is just given by the pure CP violating effect and the ordinary matter effect. The FDNI effect is negligibly small just as the FCNI effect and is not shown in Fig.12.

IV Conclusions and discussions

In this paper we have studied the effects of non-standard neutrino-matter interactions on the standard mass-induced oscillation probabilities and the CP violating effects. The non-standard interactions are introduced in the flavor-changing neutrino interaction (FCNI) and the flavor-diagonal one (FDNI) as sub-leading effects in the $\nu_\mu - \nu_\tau$ sector and $\nu_e - \nu_\mu$ sector in order to investigate their effects in $\nu_\mu \to \nu_\tau$ and $\nu_\mu \to \nu_e$ oscillations, respectively, at the baselines of $L = 730$

and 300 km. By using the values of FCNI and FDNI parameters allowed by the atmospheric neutrino oscillation analyses, in $\nu_\mu \to \nu_\tau$ oscillation at $L = 730$ km the FCNI contribution has proved to dominate the CP violating effect and survive significantly in the energy region where all the others of pure CP violating effect, ordinary matter effect and FDNI contribution fall. In $\nu_\mu \to \nu_e$ oscillation at $L = 300$ km, the FCNI and FDNI contributions are negligibly small due to the stringent constraints on FCNI from the bounds on various lepton flavor violating processes and on FDNI from the limits on lepton universality violation.

These results show that the non-standard neutrino-matter interations, especially the flavor-changing neutrino interaction, could be detected in the CP violating effect in $\nu_\mu \to \nu_\tau$ oscillation at the neutrino energies where both the pure CP violating effect and the ordinary matter effect fall, for example, above 4 GeV at $L = 730$ km.[1]

---

[1] After the completion of this work, Prof. Branco informed us that they studied the effect of the addition of a new isosinglet charged lepton inspired by extra dimensions to the standard spectrum on the CP asymmetries in neutrino oscillations in $\nu_e - \nu_\mu$ and $\nu_\mu - \nu_\tau$ channels and its detectability at future neutrino factories. [25]

Appendix A: Oscillation probability with NSNI in $\nu_\mu - \nu_\tau$ sector

Here we present the oscillation probability of Eq.(8) with Eq.(19) taken in Eq.(18).

$$
\begin{aligned}
P\ &(\nu_\alpha \to \nu_\beta; L) \\
= \ &\delta_{\beta\alpha}\Big[\, 1 - 4\sin^2\left(\frac{\Delta m^2_{31}L}{4E}\right)\Big\{|U_{\alpha 3}|^2\big[\, 1 - 2\frac{a}{\Delta m^2_{31}}(|U_{e3}|^2 - \delta_{\alpha e}) \\
&- 2\frac{\epsilon' b}{\Delta m^2_{31}}(|U_{\tau 3}|^2 - \delta_{\alpha\tau})\,\big] - \frac{2}{\Delta m^2_{31}}\mathrm{Re}(\epsilon b U^*_{\mu 3}U_{\tau 3})(2|U_{\alpha 3}|^2 - \delta_{\alpha\mu} - \delta_{\alpha\tau})\Big\} \\
&- 2\sin\left(\frac{\Delta m^2_{31}L}{2E}\right)|U_{\alpha 3}|^2\Big\{\frac{aL}{2E}|U_{e3}|^2 + 2\frac{L}{2E}\mathrm{Re}(\epsilon b U^*_{\mu 3}U_{\tau 3}) + \frac{\epsilon' b L}{2E}|U_{\tau 3}|^2\Big\}\,\Big] \\
&+ 4\sin^2\left(\frac{\Delta m^2_{31}L}{4E}\right)\Big[\,|U_{\alpha 3}|^2|U_{\beta 3}|^2\{1 - 2\frac{a}{\Delta m^2_{31}}(2|U_{e3}|^2 - \delta_{\alpha e} - \delta_{\beta e}) \\
&- 2\frac{\epsilon' b}{\Delta m^2_{31}}(2|U_{\tau 3}|^2 - \delta_{\alpha\tau} - \delta_{\beta\tau})\} - \frac{2}{\Delta m^2_{31}}\mathrm{Re}(\epsilon b U^*_{\mu 3}U_{\tau 3})\{4|U_{\alpha 3}|^2|U_{\beta 3}|^2 \\
&- |U_{\alpha 3}|^2(\delta_{\beta\mu} + \delta_{\beta\tau}) - |U_{\beta 3}|^2(\delta_{\alpha\mu} + \delta_{\alpha\tau})\}\,\Big] + 2\frac{\Delta m^2_{31}L}{2E}\sin\left(\frac{\Delta m^2_{31}L}{2E}\right) \\
&\times\Big[\,\frac{\Delta m^2_{21}}{\Delta m^2_{31}}\mathrm{Re}(U_{\beta 3}U^*_{\beta 2}U^*_{\alpha 3}U_{\alpha 2}) + \frac{a}{\Delta m^2_{31}}\{\delta_{\alpha e}\delta_{\beta e}|U_{e3}|^2 + |U_{\alpha 3}|^2|U_{\beta 3}|^2(2|U_{e3}|^2 \\
&- \delta_{\alpha e} - \delta_{\beta e})\} + \frac{\epsilon' b}{\Delta m^2_{31}}\{\delta_{\alpha\tau}\delta_{\beta\tau}|U_{\tau 3}|^2 + |U_{\alpha 3}|^2|U_{\beta 3}|^2(2|U_{\tau 3}|^2 - \delta_{\alpha\tau} - \delta_{\beta\tau})\} \\
&+ \frac{1}{\Delta m^2_{31}}\mathrm{Re}(\epsilon b U^*_{\mu 3}U_{\tau 3})\{\delta_{\alpha\mu}\delta_{\beta\tau} + \delta_{\alpha\tau}\delta_{\beta\mu} + 4|U_{\alpha 3}|^2|U_{\beta 3}|^2 \\
&- |U_{\alpha 3}|^2(\delta_{\beta\mu} + \delta_{\beta\tau}) - |U_{\beta 3}|^2(\delta_{\alpha\mu} + \delta_{\alpha\tau})\}\,\Big] + 4\frac{\Delta m^2_{31}L}{2E}\sin^2\left(\frac{\Delta m^2_{31}L}{4E}\right) \\
&\times\Big[\,\frac{\Delta m^2_{21}}{\Delta m^2_{31}}\mathrm{Im}(U_{\beta 3}U^*_{\beta 2}U^*_{\alpha 3}U_{\alpha 2}) + \frac{1}{\Delta m^2_{31}}\mathrm{Im}(\epsilon b U^*_{\mu 3}U_{\tau 3})\{\delta_{\alpha\mu}\delta_{\beta\tau} - \delta_{\alpha\tau}\delta_{\beta\mu} \\
&+ |U_{\alpha 3}|^2(\delta_{\beta\mu} - \delta_{\beta\tau}) - |U_{\beta 3}|^2(\delta_{\alpha\mu} - \delta_{\alpha\tau})\}\,\Big]. \qquad \text{(A1)}
\end{aligned}
$$

Appendix B: Oscillation probability with NSNI in $\nu_e - \nu_\mu$ sector

Here we present the oscillation probability of Eq.(8) with Eq.(26) taken in Eq.(18).

$$
\begin{aligned}
P\ & (\nu_\alpha \rightarrow \nu_\beta; L) \\
= \ & \delta_{\beta\alpha}\Big[\, 1 - 4\sin^2\left(\frac{\Delta m^2_{31}L}{4E}\right)\Big\{|U_{\alpha 3}|^2[\, 1 - 2\frac{a}{\Delta m^2_{31}}(|U_{e3}|^2 - \delta_{\alpha e}) \\
& - 2\frac{\eta' b}{\Delta m^2_{31}}(|U_{\mu 3}|^2 - \delta_{\alpha\mu})\,] - \frac{2}{\Delta m^2_{31}}\mathrm{Re}(\eta b U^*_{e3}U_{\mu 3})(2|U_{\alpha 3}|^2 - \delta_{\alpha\mu} - \delta_{\alpha e})\Big\} \\
& - 2\sin\left(\frac{\Delta m^2_{31}L}{2E}\right)|U_{\alpha 3}|^2\Big\{\frac{aL}{2E}|U_{e3}|^2 + 2\frac{L}{2E}\mathrm{Re}(\eta b U^*_{e3}U_{\mu 3}) + \frac{\eta' b L}{2E}|U_{\mu 3}|^2\Big\}\,\Big] \\
& + 4\sin^2\left(\frac{\Delta m^2_{31}L}{4E}\right)\Big[\,|U_{\alpha 3}|^2|U_{\beta 3}|^2\{1 - 2\frac{a}{\Delta m^2_{31}}(2|U_{e3}|^2 - \delta_{\alpha e} - \delta_{\beta e}) \\
& - 2\frac{\eta' b}{\Delta m^2_{31}}(2|U_{\mu 3}|^2 - \delta_{\alpha\mu} - \delta_{\beta\mu})\} - \frac{2}{\Delta m^2_{31}}\mathrm{Re}(\eta b U^*_{e3}U_{\mu 3})\{4|U_{\alpha 3}|^2|U_{\beta 3}|^2 \\
& - |U_{\alpha 3}|^2(\delta_{\beta e} + \delta_{\beta\mu}) - |U_{\beta 3}|^2(\delta_{\alpha e} + \delta_{\alpha\mu})\}\,\Big] + 2\frac{\Delta m^2_{31}L}{2E}\sin\left(\frac{\Delta m^2_{31}L}{2E}\right) \\
& \times \Big[\,\frac{\Delta m^2_{21}}{\Delta m^2_{31}}\mathrm{Re}(U_{\beta 3}U^*_{\beta 2}U^*_{\alpha 3}U_{\alpha 2}) + \frac{a}{\Delta m^2_{31}}\{\delta_{\alpha e}\delta_{\beta e}|U_{e3}|^2 + |U_{\alpha 3}|^2|U_{\beta 3}|^2(2|U_{e3}|^2 \\
& - \delta_{\alpha e} - \delta_{\beta e})\} + \frac{\eta' b}{\Delta m^2_{31}}\{\delta_{\alpha\mu}\delta_{\beta\mu}|U_{\mu 3}|^2 + |U_{\alpha 3}|^2|U_{\beta 3}|^2(2|U_{\mu 3}|^2 - \delta_{\alpha\mu} - \delta_{\beta\mu})\} \\
& + \frac{1}{\Delta m^2_{31}}\mathrm{Re}(\eta b U^*_{e3}U_{\mu 3})\{\delta_{\alpha e}\delta_{\beta\mu} + \delta_{\alpha\mu}\delta_{\beta e} + 4|U_{\alpha 3}|^2|U_{\beta 3}|^2 \\
& - |U_{\alpha 3}|^2(\delta_{\beta e} + \delta_{\beta\mu}) - |U_{\beta 3}|^2(\delta_{\alpha e} + \delta_{\alpha\mu})\}\,\Big] + 4\frac{\Delta m^2_{31}L}{2E}\sin^2\left(\frac{\Delta m^2_{31}L}{4E}\right) \\
& \times \Big[\,\frac{\Delta m^2_{21}}{\Delta m^2_{31}}\mathrm{Im}(U_{\beta 3}U^*_{\beta 2}U^*_{\alpha 3}U_{\alpha 2}) + \frac{1}{\Delta m^2_{31}}\mathrm{Im}(\eta b U^*_{e3}U_{\mu 3})\{\delta_{\alpha e}\delta_{\beta\mu} - \delta_{\alpha\mu}\delta_{\beta e} \\
& + |U_{\alpha 3}|^2(\delta_{\beta e} - \delta_{\beta\mu}) - |U_{\beta 3}|^2(\delta_{\alpha e} - \delta_{\alpha\mu})\}\,\Big].
\end{aligned}
\tag{B1}
$$

References

[1] Kamiokande Collaboration, K.S. Hirata et al., Phys. Lett. B **205**, 416(1988); Kamiokande Collaboration, Y. Fukuda et al., Phys. Lett. B **335**, 237(1994); IMB Collaboration, D. Casper et al., Phys. Rev. Lett. **66**, 2561(1991); IMB Collaboration, R. Becker-Szendy et al., Phys. Rev. D **46**, 3720(1992); Soudan2 Collaboration, W.W.M. Allison et al., Phys. Lett. B **391**, 491 (1997); **449**, 137 (1999); Super-Kamiokande Collaboration, Y. Fukuda et al., Phys. Lett. B **433**, 9 (1998); **436**, 33 (1998); Phys. Rev. Lett. **82**, 2644 (1999); MACRO Collaboration, M. Ambrosio et al., Phys. Lett. B **434**, 451 (1998); **478**, 5 (2000).

[2] Super-Kamiokande Collaboration, Y. Fukuda et al. Phys. Rev. Lett. **81**, 1562 (1998).

[3] Homestake Collaboration, B.T. Cleveland et al., Astrophys. J. **496**, 505 (1988); K. Lande et al., Nucl. Phys. B (Proc. Suppl.) **91**, 50 (2001); SAGE Collaboration, J.N. Abdurashitov et al., Phys. Rev. C **60**, 055801 (1999); GALLEX Collaboration, W. Hampel et al., Phys. Lett. B **447**, 127 (1999); GNO Collaboration, M. Altmann et al., Phys. Lett. B **490**, 16 (2000); Kamiokande Collaboration, Y. Fukuda et al., Phys. Rev. Lett. **77**, 1683 (1996); Super-Kamiokande Collaboration, Y. Fukuda et al., Phys. Rev. Lett. **81**, 1158 (1998); Erratum **81**, 4279 (1998); **82**, 1810 (1999); **82**, 2430 (1999); Super-Kamiokande Collaboration, S. Fukuda et al., Phys. Rev. Lett. **86**, 5651 (2001); SNO Collaboration, Q.R. Ahmad et al. , Phys. Rev. Lett. **87**, 071301 (2001); **89**, 011301 (2002); **89** 011302 (2002).

[4] J.N. Bahcall, P.I.Krastev, and A. Yu. Smirnov, Phys. Rev. D **58**, 096016 (1998); G. Fogli, E. Lisi, D. Montanino, and A. Palazzo, *ibid.* **62**, 013002 (2000); **64**, 093007 (2001); J.N. Bahcall, M.C. Gonzalez-Garcia, and C. Peña-

Garay, JHEP **0108**, 014 (2001); A. Bandyopadhyay, S. Choubey, S. Goswami, and K. Kar, Phys. Lett. B **519**, 83 (2001).

[5] S.P. Mikheyev and A.Yu. Smirnov, Sov. J. Nucl. Phys. **42**, 913 (1985); Nuovo Cimento **C9**, 17 (1986); L. Wolfenstein, Phys. Rev. D **17**, 2369 (1978).

[6] Z. Maki, M. Nakagawa, and S. Sakata, Prog. Theor. Phys. **28**, 870 (1962).

[7] M. Apollonio et al., Phys. Lett. B **420**, 397 (1998); **466**, 415 (1999).

[8] C. Athanassopoulos et al., Phys. Rev. Lett. **75**, 2650 (1995); **77**, 3082(1996); **81**, 1774(1998); R.L. Imlay (LSND Collaboration), in *ICHEP 2000*, Proceeindings of the 30th International Conference on High Energy Physics, Osaka, July 2000, eds. C.S. Lim and T. Yamanaka, p950.

[9] Wolfenstein [5]; L. Wolfenstein, Phys. Rev. D **20**, 2634 (1979).

[10] M.M. Guzzo, A. Masiero, and S.T. Petcov, Phys. Lett. B **260**, 154 (1991); E. Roulet, Phys. Rev. D **44**, 935 (1991); V. Barger, R.J.N. Phillips, and K. Whisnant, Phys. Rev. D **44**, 1629 (1991).

[11] S. Bergmann, M.M. Guzzo, P.C. de Holanda, P.I. Krastev, and H. Nunokawa, Phys. Rev. D **62**, 073001 (2000).

[12] S. Bergmann, Nucl. Phys. B **515**, 363 (1998); Z. Berezhiani, R.S. Raghavan, and A. Rossi, Nucl. Phys. B **638**, 62 (2002).

[13] E. Ma and P. Roy, Phys. Rev. Lett. **80**, 4637 (1998).

[14] M.C. Gonzalez-Garcia, M.M. Guzzo, P.I. Krastev, H. Nunokawa, O.L.G. Peres, V. Pleitez, J.W.F. Valle, and R. Zukanovich Funchal, Phys. Rev. Lett. **82**, 3202 (1999); P. Lipari and M. Lusignoli, Phys. Rev. D **60**, 013003 (1999); N. Fornengo, M.C. Gonzalez-Garcia, and J.W.F. Valle, JHEP **0007**, 006 (2000).

[15] S. Bergmann, Y. Grossman, and D.M. Pierce, Phys. Rev. D **61**, 053005 (2000).

[16] N. Fornengo, M. Maltoni, R. Tomàs Bayo, and J.W. Valle, Phys. Rev. D **65**, 013010 (2001) (arXiv:hep-ph/0108043); M. Maltoni, Nucl. Phys. Proc. Suppl. **114**, 191 (2003).

[17] A.M. Gago, M.M. Guzzo, H. Nunokawa, W.J.C. Teves, and R. Zukanovich Funchal, Phys. Rev. D **64**, 073003 (2001).

[18] P. Huber and J.W.F. Valle, Phys. Lett. B **523**, 151 (2001); P. Huber, T. Schwetz, and J.W.F. Valle, Phys. Rev. Lett. **88**, 101804 (2002).

[19] M. Campanelli and A. Romanino, hep-ph/0207350.

[20] H. Nunokawa, Nucl. Instrum. Meth. A **472**, 443 (2000).

[21] M.C. Gonzalez-Garcia, Y. Grossman, A. Gusso, and Y. Nir, Phys. Rev. D **64**, 096006 (2001); T. Ota, J. Sato, and N. Yamashita, Phys. Rev. D **65**, 093015 (2002); P. Huber, T. Schwetz, and J.W.F. Valle, Phys. Rev. D **66**, 013006 (2002).

[22] J. Arafune, M. Koike, and J. Sato, Phys. Rev. D **56**, 3093 (1997); **60**, 119905(E) (1999).

[23] S. Bergmann and Y. Grossman, Phys. Rev. D **59**, 093005 (1999).

[24] Super-Kamiokande Collaboration, S. Fukuda et al. Phys. Rev. Lett. **86**, 5656 (2001).

[25] G.C. Branco, D. Delépine, B. Nobre, and J. Santiago, Nucl. Phys. B **657**, 355 (2003).

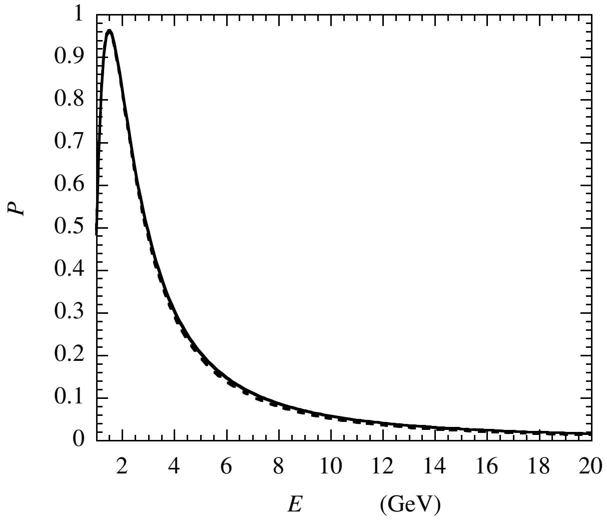

Figure 1: $\nu_\mu \to \nu_\tau$ oscillation probability for the neutrino energy range $E = 1 - 20$ GeV at the baseline of $L = 730$ km, with the NSNI in $\nu_\mu - \nu_\tau$ sector. The solid line is the one with all of the ordinary, FCNI and FDNI matter effects included, for $|\epsilon| = 0.01, \epsilon' = 0.02, \phi = 0$ for the phase of ϵ, $\delta = \pi/2$ for the phase of $U, \Delta m^2_{21} = 7.3 \times 10^{-5}$ eV^2, and $\Delta m^2_{31} = 2.5 \times 10^{-3}$eV^2 (> 0). The dashed line is the one without any matter effects.

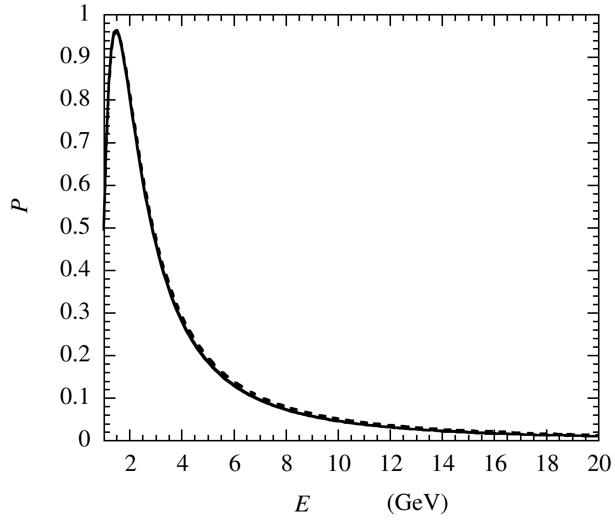

Figure 2: $\nu_\mu \to \nu_\tau$ oscillation probability for the neutrino energy range $E = 1-20$ GeV at $L = 730$ km with all of the ordinary, FCNI and FDNI matter effects included (solid line) and without any matter effects (dashed line). The parameter values are the same as in Fig.1 except for $\phi = \pi$.

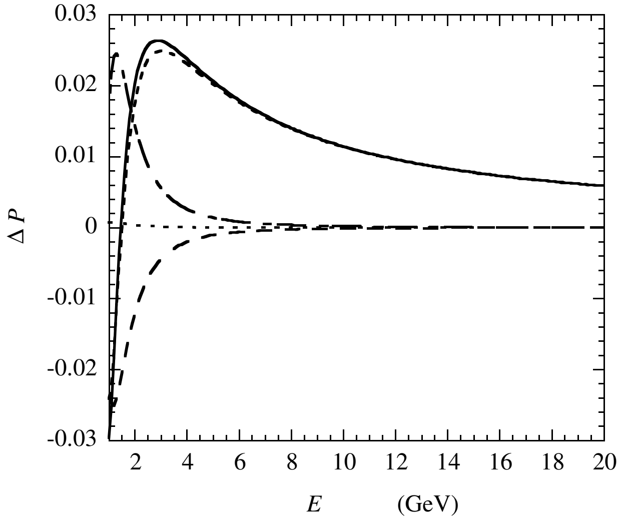

Figure 3: The CP violating effect in $\nu_\mu \to \nu_\tau$ oscillation for the neutrino energy range $E = 1 - 20$ GeV at $L = 730$ km, with the NSNI in $\nu_\mu - \nu_\tau$ sector. The dash-dotted line is the pure CP violating effect. The long-dashed, short-dashed and dotted lines are the fake CP violating effects due to the ordinary, FCNI and FDNI matter effects, respectively. The solid line is the total CP violating effect with the pure and fake ones. The parameter values are $|\epsilon| = 0.01, \epsilon' = 0.02, \phi = 0, s_{12} = 0.54, s_{23} = 0.707, s_{13} = 0.14, \delta = \pi/2, \Delta m^2_{21} = 7.3 \times 10^{-5}$ eV^2, and $\Delta m^2_{31} = 2.5 \times 10^{-3}$eV^2 (> 0).

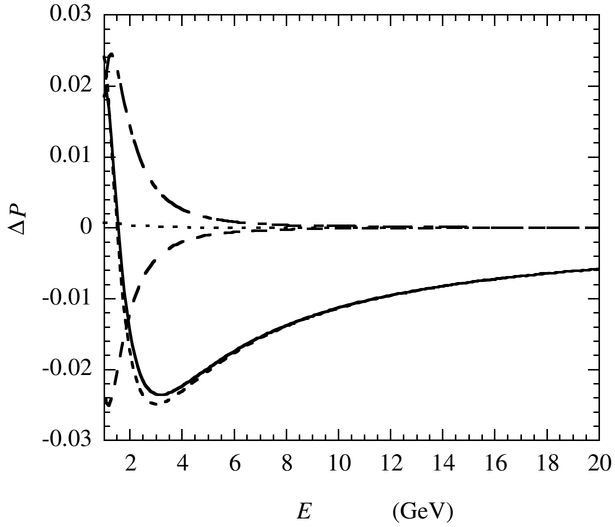

Figure 4: The CP violating effect in $\nu_\mu \to \nu_\tau$ oscillation at $L = 730$ km with the same parameter values as in Fig.3 except for $\phi = \pi$. The lines represent the same ones as in Fig.3.

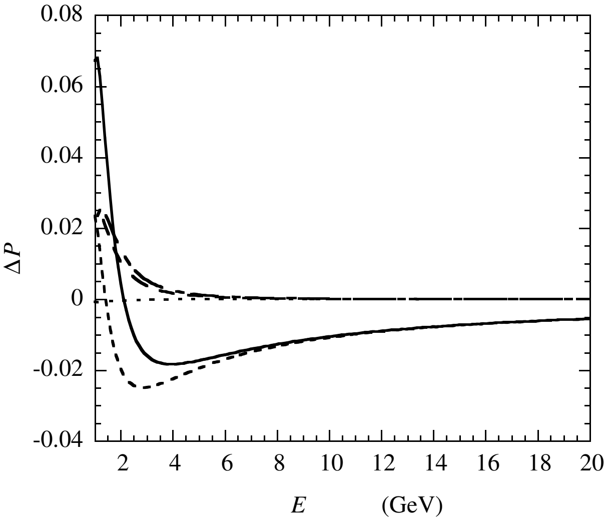

Figure 5: The CP violating effect in $\nu_\mu \rightarrow \nu_\tau$ oscillation at $L = 730$ km with the same parameter values as in Fig.3 except for $\Delta m^2_{31} < 0$. The lines represent the same ones as in Fig.3.

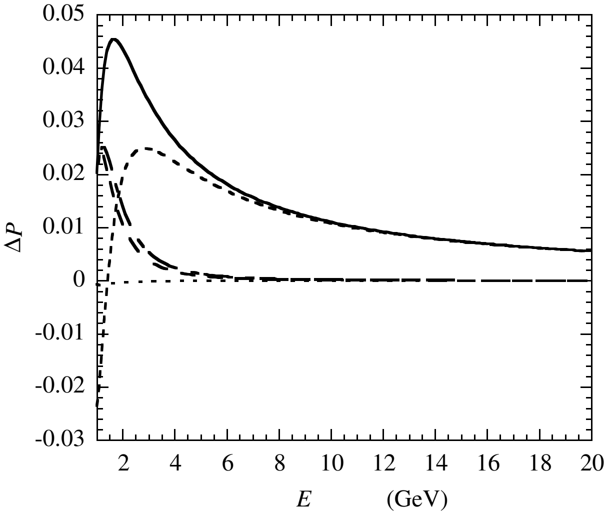

Figure 6: The CP violating effect in $\nu_\mu \to \nu_\tau$ oscillation at $L = 730$ km with the same parameter values as in Fig.3 except for $\phi = \pi$ and $\Delta m^2_{31} < 0$. The lines represent the same ones as in Fig.3.

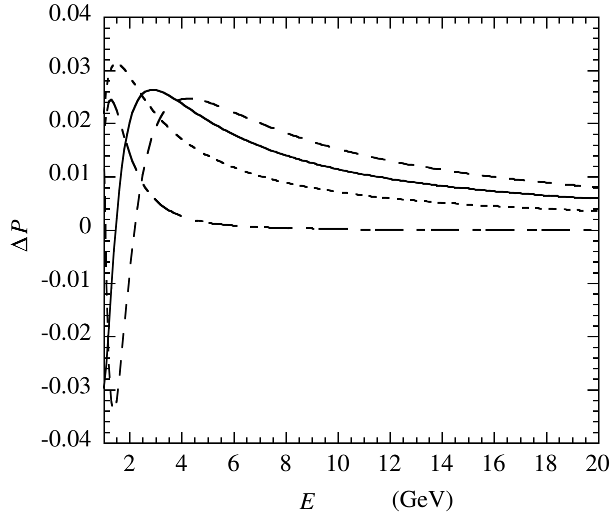

Figure 7: The dependence on Δm_{31}^2 of the total CP violating effect in $\nu_\mu \to \nu_\tau$ oscillation at $L = 730$ km. The short-dashed, solid, and long-dashed lines are for $\Delta m_{31}^2 = 1.5 \times 10^{-3}, 2.5 \times 10^{-3}$, and 3.5×10^{-3} eV^2, respectively. The other mixing parameters are the same as in Fig.3. The dash-dotted line represents the pure CP violating effect without the FCNI and FDNI for $\Delta m_{31}^2 = 2.5 \times 10^{-3}$ eV^2.

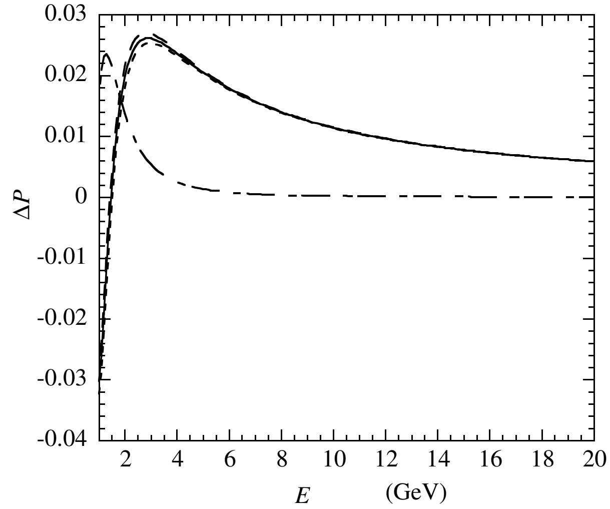

Figure 8: The dependence on Δm_{21}^2 of the total CP violating effect in $\nu_\mu \rightarrow \nu_\tau$ oscillation at $L = 730$ km. The short-dashed, solid, and long-dashed lines are for $\Delta m_{21}^2 = 6 \times 10^{-5}, 7 \times 10^{-5}$, and 8×10^{-5} eV^2, respectively. The other mixing parameters are the same as in Fig.3. The dash-dotted line represents the pure CP violating effect without the FCNI and FDNI for $\Delta m_{21}^2 = 7 \times 10^{-5}$ eV^2.

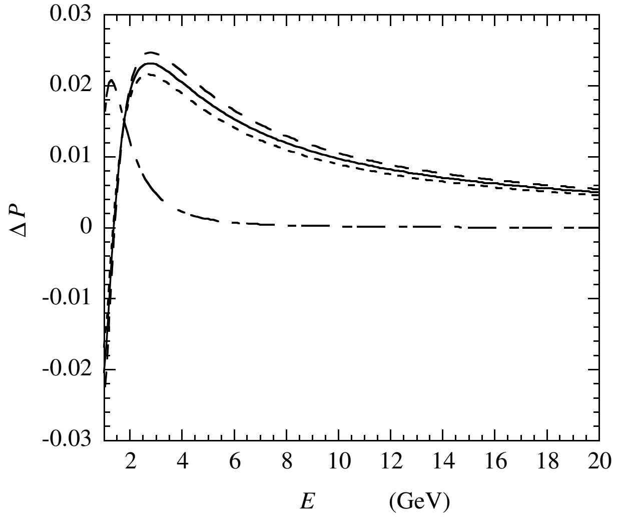

Figure 9: The dependence on the mixing angle s_{23} of the total CP violating effect in $\nu_\mu \to \nu_\tau$ oscillation at $L = 730$ km. The short-dashed, solid, and long-dashed lines are for $s_{23} = 0.55, 0.60$ and 0.65, respectively. The other mixing parameters are the same as in Fig.3. The dash-dotted line represents the pure CP violating effect without the FCNI and FDNI for $s_{23} = 0.65$.

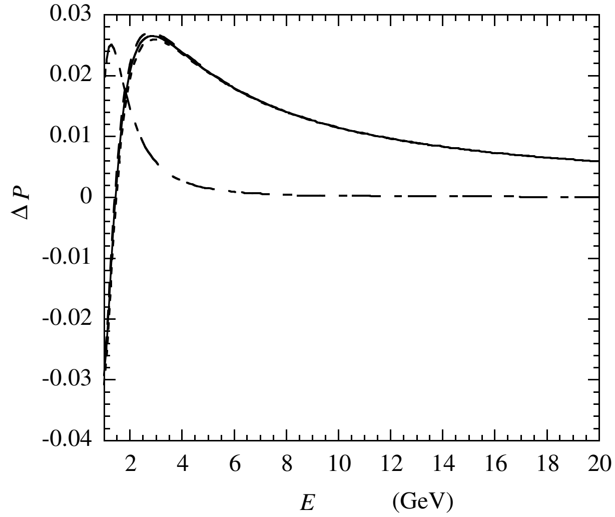

Figure 10: The dependence on the mixing angle s_{12} of the total CP violating effect in $\nu_\mu \longrightarrow \nu_\tau$ oscillation at $L = 730$ km. The short-dashed, solid, and long-dashed lines are for $s_{12} = 0.50, 0.55$ and 0.60, respectively. The other mixing parameters are the same as in Fig.3. The dash-dotted line represents the pure CP violating effect without the FCNI and FDNI for $s_{12} = 0.55$.

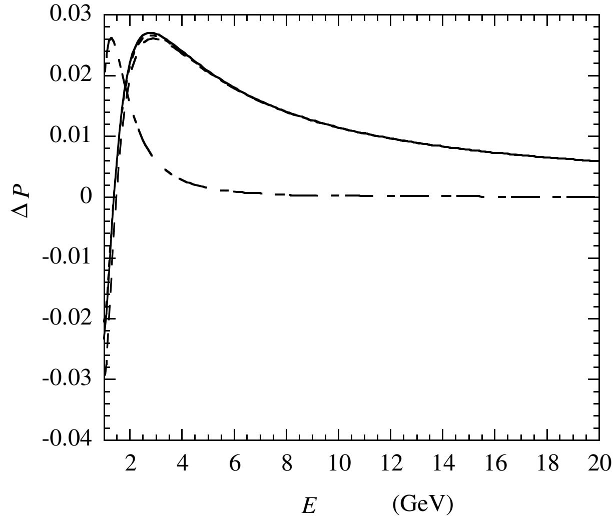

Figure 11: The dependence on the mixing angle s_{13} of the total CP violating effect in $\nu_\mu \longrightarrow \nu_\tau$ oscillation at $L = 730$ km. The short-dashed, solid, and long-dashed lines are for $s_{13} = 0.05, 0.10$ and 0.15, respectively. The other mixing parameters are the same as in Fig.3. The dash-dotted line represents the pure CP violating effect without the FCNI and FDNI for $s_{13} = 0.15$.

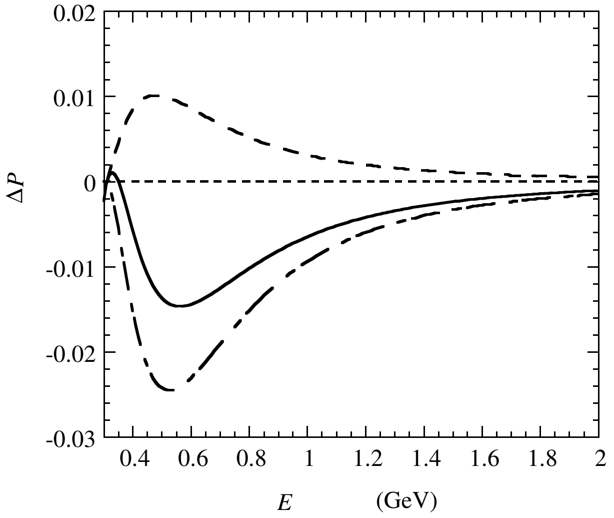

Figure 12: The CP violating effect in $\nu_\mu \to \nu_e$ oscillation for the neutrino energy range $E = 0.3 - 2$ GeV at $L = 300$ km, with the NSNI in $\nu_e - \nu_\mu$ sector. The dash-dotted line is the pure CP violating effect. The long-dashed and short-dashed lines are the fake CP violating effects due to the ordinary and FCNI matter effects, respectively. The solid line is the total CP violating effect with the pure and fake ones. The parameter values are $|\eta| = 7\times10^{-5}, \eta' = 0.01, \gamma = \pi/2, s_{12} = 0.54, s_{23} = 0.707, s_{13} = 0.14, \delta = \pi/2, \Delta m^2_{21} = 7.3 \times 10^{-5}$ eV^2, and $\Delta m^2_{31} = 2.5 \times 10^{-3}$eV^2 (> 0).